

LA-UR-17-22363 (Accepted Manuscript)

## Resonant Ultrasound Spectroscopy studies of Berea sandstone at high temperature

Davis, Eric Sean  
Pantea, Cristian  
Sturtevant, Blake  
Sinha, Dipen N.

Provided by the author(s) and the Los Alamos National Laboratory (2017-08-04).

**To be published in:** Journal of Geophysical Research: Solid Earth

**DOI to publisher's version:** 10.1002/2016JB013410

**Permalink to record:** <http://permalink.lanl.gov/object/view?what=info:lanl-repo/lareport/LA-UR-17-22363>

**Disclaimer:**

Approved for public release. Los Alamos National Laboratory, an affirmative action/equal opportunity employer, is operated by the Los Alamos National Security, LLC for the National Nuclear Security Administration of the U.S. Department of Energy under contract DE-AC52-06NA25396. Los Alamos National Laboratory strongly supports academic freedom and a researcher's right to publish; as an institution, however, the Laboratory does not endorse the viewpoint of a publication or guarantee its technical correctness.

## **Resonant Ultrasound Spectroscopy Studies of Berea Sandstone at High Temperature**

Eric S. Davis, Blake T. Sturtevant, Dipen N. Sinha, and Cristian Pantea, Materials Physics and Applications, MPA-11, Los Alamos National Laboratory, Los Alamos, New Mexico, USA.

Corresponding Author: Cristian Pantea, Materials Physics Applications, MPA-11, MS D429, Los Alamos National Laboratory, Los Alamos, NM 87545, USA. ([pantea@lanl.gov](mailto:pantea@lanl.gov))

1      **Key Points.**

2      •    Elastic properties of Berea sandstone were studied at high temperatures  
3      •    Berea sandstone exhibits anomalous elastic behavior between 375 and 478 K  
4      •    Room temperature RUS bulk modulus measurements agree well with literature

5

6      **Abstract.** Resonant Ultrasound Spectroscopy was used to determine the elastic moduli of Berea  
7      sandstone from room temperature to 478K. Sandstone is a common component of oil reservoirs,  
8      and the temperature range was chosen to be representative of typical downhole conditions, down  
9      to about 8 km. In agreement with previous works, Berea sandstone was found to be relatively  
10     soft with a bulk modulus of approximately 6 GPa as compared to 37.5 GPa for  $\alpha$ -Quartz at room  
11     temperature and pressure. It was found that Berea sandstone undergoes a ~17% softening in bulk  
12     modulus between room temperature and 385 K, followed by an abnormal behavior of similar  
13     stiffening between 385 K and 478 K.

14     **Index Terms.**

15     3909 Elasticity and anelasticity,

16     3999 General or miscellaneous

17     5102 Acoustic properties

18     **Key Words.**

19     RUS, Berea sandstone, elastic properties

20

21

22

23

24

25

26

27

29 **1. Introduction**

30 Understanding the mechanical properties of rocks beneath Earth's surface, at  
 31 temperatures typically found in oil wells, is of great importance to the oil/gas and geothermal  
 32 industry. This knowledge has become even more important with the recent rise of hydraulic  
 33 fracturing (fracking) as a preferred method for oil and gas extraction. Sandstone is commonly  
 34 found in oil and gas reservoirs [Slatt, 2014] and detailed calculations based on the mechanical  
 35 properties of the reservoir's constituent materials are needed to safely and efficiently extract oil  
 36 or gas. This requirement creates a great need to determine the elastic properties of the sandstone  
 37 not only at room temperature, but also at higher temperatures to simulate downhole conditions as  
 38 temperatures quickly rise with increased drilling depth at a rate of approximately 25 kelvin per  
 39 kilometer [Finger and Blankenship, 2010].

40 Several earlier studies, briefly described here, were performed on sandstones in order to  
 41 determine their mechanical properties under different conditions of pressures and temperatures.  
 42 Ulrich and Darling performed a qualitative study on the elastic properties dependence with  
 43 temperature for Berea sandstone. The temperature range covered was room temperature to about  
 44 8 K. They showed the existence of a hysteresis in elastic properties with cooling vs warming, and  
 45 also the presence of an anomalous behavior which indicates that Berea sandstone is softening  
 46 with decrease in temperature between 200 K and 60 K. [Ulrich and Darling, 2001]. Liang et al.  
 47 discovered that salt rock strength is affected very little by strain rate and that there is a  
 48 logarithmic relationship between deformation modulus and loading strain rate [Liang et al.,  
 49 2011]. Ten Cate and Shankland explored slow dynamics in Berea sandstone and found that it has  
 50 a strong memory of strain history and hysteresis in resonant frequencies with changing strain  
 51 amplitude [Ten Cate and Shankland, 1996]. Costin and Holcomb found that cyclic loading can  
 52 induce microcrack damage in rocks and cause specimen failure that is inconsistent with results  
 53 extrapolated from static tests. Additionally, Costin and Holcomb found that high stress can  
 54 destroy discrete memory in rock specimens and reduce stress cycle hysteresis [Costin and  
 55 Holcomb, 1981]. Rocks, and particularly sandstone, exhibit several unusual elastic responses to  
 56 stress that include nonclassical attenuation, stress-strain hysteresis, slow dynamics, and high  
 57 vibrational energy loss due to internal defects [Johnson et al., 1999; Lebedev, 2002]. These  
 58 features, combined with the acoustic nonlinearity of the material that is due to the bond system  
 59 controlling the elastic properties rather than the grains, result in rock being an extremely difficult  
 60 material to study mechanically [Nobili et al., 2005]. These materials merit further study as their  
 61 mechanical behavior have a strong temperature dependence. Several factors, such as  
 62 temperature, pressure, composition, porosity, moisture etc., are known to affect the elastic  
 63 properties of porous materials [Zhang and Bentley, 2003]. Berea sandstone is a relatively soft,  
 64 porous material that is highly attenuating to sound and attributes most of its mechanical  
 65 properties to quartz, which is its major constituent. Berea sandstone has a porosity of 13% to

66 23% and is composed of 93.13% silica, 3.86% alumina, 0.54% ferrous oxide, 0.25% magnesia,  
67 0.11% ferric oxide, and 0.10% calcium oxide ([www.bereasandstonecores.com](http://www.bereasandstonecores.com)). Berea sandstone  
68 exhibits no known temperature induced phase transitions between room temperature and ~846 K.

69 Most past studies of Berea sandstone's elastic properties have used pulse-echo, or  
70 transmit-receive approaches [Winkler, 1983; Green and Wang, 1994]. Harris and Wang used  
71 Differential Acoustic Resonance Spectroscopy (DARS) which allows for a wide variety of  
72 sample shapes and quick sample preparation and works by measuring the resonance shift  
73 between a fluid-filled cavity and the same cavity with a sample placed inside. This technique has  
74 allowed for very low frequency sound speed measurements on rock samples with highly  
75 irregular shapes and extremely small dimensions with results comparable to literature values  
76 [Harris *et al.*, 2005; Wang *et al.*, 2012]. Hart and Wang measured the poroelastic moduli of  
77 Berea sandstone using static stress-strain measurements under varying pore pressure conditions  
78 [Hart and Wang, 1995]. Ulrich used Resonant Ultrasound Spectroscopy (RUS) to perform a  
79 qualitative study of the behavior of Berea sandstone at low temperatures [Ulrich and Darling,  
80 2001], while Ten Cate [Ten Cate and Shankland, 1996] and Johnson [Johnson *et al.*, 2004], used  
81 a variation of RUS, Nonlinear RUS (NRUS) to investigate its slow dynamics. Renaud *et al.*  
82 [Renaud *et al.*, 2013] used a dynamic acousto-elastic method to investigate the elasticity of dry  
83 Berea sandstone as a function of applied low-frequency axial strain.

84 This paper focuses exclusively on high temperature effects, using RUS, a technique  
85 known to provide elastic constants with high accuracy [Migliori and Sarrao, 1997] The RUS  
86 technique is treated exhaustively in Ref [Migliori and Sarrao, 1997] but is described here briefly  
87 for completeness. RUS is used to accurately and nondestructively extract the elastic moduli of a  
88 small solid object of well-defined geometry using the material's natural mechanical resonances.  
89 In RUS, a swept frequency acoustic signal is applied to the sample through a piezoelectric  
90 transducer while the mechanical response is recorded using a second transducer in contact with  
91 the sample. This technique can be applied to a wide variety of sample types and geometries with  
92 very little material needed and provides the highest accuracy for determination of elastic  
93 constants, with typical accuracies of 0.5-1.0% for compressional moduli and .02% for shear  
94 moduli from fits with a 0.1-0.2% RMS error [Migliori and Sarrao, 1997; Pandey and Schreuer,  
95 2012; Liu *et al.*, 2010; Sedmák *et al.*, 2013]. Additionally, RUS is capable of measurements over  
96 a significantly large temperature and pressure range which is important for simulating inner-earth  
97 conditions and elucidating effects of changing environment on the mechanical properties of  
98 materials.

## 99 2. Experimental

100 The Berea sandstone sample used in our study was cut and prepared into a rectangular  
101 parallelepiped with the dimensions 9.13 x 8.32 x 6.65 mm<sup>3</sup>. The small sample size was chosen to  
102 avoid low frequency resonances which would couple to other parts of the experimental  
103 apparatus. Small samples have the added advantage that they are effectively isotropic, a feature

104 that is not necessarily true for a larger sedimentary sample [Sayers *et al.*, 1990]. As the largest  
105 wavelength used in this study (12.55mm) is several magnitudes larger than the average grain size  
106 of Berea sandstone, isotropy can be assumed for the Berea sample. The sample was mounted  
107 between two Boston PiezoOptics, 6 x 2 x 3.25 mm, 1 MHz, 36° Y-cut (P-wave or longitudinally-  
108 polarized) LiNbO<sub>3</sub> piezoelectric transducers. In theory, RUS assumes free boundary conditions  
109 for the sample. Experimentally, this is achieved by using point contacts between the sample and  
110 the transducers. Corner mounting of the transducers was attempted to achieve this condition and  
111 to reduce noise from transducer contact, but it was found that such a mounting implementation  
112 was not only impractical for the environmental conditions in this study, but also difficult to  
113 achieve from the standpoint of obtaining sufficient acoustic signal through the transducer.  
114 Consequently, the transducers were affixed with a high temperature epoxy (EPO-TEK, TM112)  
115 to the 9.13 x 6.65 mm face parallel to the 9.13 mm side of the sample (Fig. 1). The  
116 sample/transducer assembly was placed into a small-diameter tube furnace (Blue M) with a PID  
117 controller (Eurotherm 847) for precise temperature manipulation. The furnace environment  
118 initially consisted of ambient air and remained unmodified throughout the experiment except by  
119 temperature change. Near-sample temperature was obtained using a type-J thermocouple  
120 attached to a data acquisition module (MC USB-TC-AI DAQ, Measurement Computing). RUS  
121 spectra were obtained using a vector network analyzer (Bode 100, Omicron Lab) connected to a  
122 computer for data acquisition. Prior to data collection, the sample was heated to 478 K for a  
123 period of two hours to thoroughly dry the sample. After this initial baking, the sample and  
124 transducers were brought back to room temperature inside the furnace tube with both ends  
125 stuffed with quartz wool. The following day, the sample and transducer were heated to 478 K in  
126 less than an hour and then cooled to room temperature over a period of approximately 7 hours.  
127 During sample cooling, the furnace temperature was briefly (~5 minutes) stabilized every 5 K so  
128 that data could be collected. Each spectrum spanned frequencies between 50 kHz and 170 kHz  
129 with 4096 points and the network analyzer had a source power of 12.0 dBm and an IF bandwidth  
130 of 100 Hz. Each sweep took approximately four minutes, during which the furnace temperature  
131 was stable to within 1 K.

### 132 **3. Results**

133 Based on theoretical calculations, the frequency region studied here covers the first 31  
134 resonances for the sample used in this study. In order to reliably determine elastic moduli, it is  
135 generally accepted that one must have at least five resonances per elastic modulus [Migliori and  
136 Sarrao, 1997]. An isotropic polycrystalline sample, such as the one studied here, has two  
137 independent elastic moduli, requiring at least 10 resonances to be taken into account.

138 At each temperature, the RUS spectrum was analyzed using freely available RUS  
139 analysis code available at <https://nationalmaglab.org/user-facilities/dc-field/dcfield-techniques/resonant-ultrasound-dc>. As an example of the procedure used, the room temperature  
140 data analysis will be described in the next section.  
141

142 

### 3.1. Room Temperature

143 The room temperature RUS spectrum is shown in Fig. 2. The quality factor (Q),  
144 calculated here as the frequency of a peak divided by its full width at half maximum, ranged  
145 from 100-250 depending on the resonance being considered. This Q factor is in agreement with  
146 that obtained by Winkler et al. which reported a Q of ~140-170 for dry Berea sandstone at low  
147 strain amplitudes [Winkler et al., 1979]. Although Berea sandstone is highly attenuating, it can  
148 be seen in Fig. 2 that the resonant frequencies are readily identified, even with the peak  
149 broadening associated with a low Q factor and some overlapping of neighboring peaks. For  
150 correct mode identification in Berea Sandstone, we used different sets of elastic constants, either  
151 from literature [Remillieux et al., 2015; Shankland et al., 1993; Renaud et al., 2013; Winkler et  
152 al., 1979; Sayers et al., 1990], or from through-transmission experiments for both compressional  
153 and shear waves, performed in our lab. These values provide a reasonable starting guess for  
154 forward calculation of the resonant frequencies. Multiple room temperature fittings were  
155 performed with a wide variety of  $C_{ij}$  values until error minimization between computed and  
156 experimental resonances was achieved. Experimental modes corresponding strongly with their  
157 calculated room temperature counterparts can then be tracked with temperature as they exhibit  
158 only small shifts between successive temperature steps.

159 Table 1 presents the results obtained from a fit to the room temperature experimental  
160 resonance data. The fit was calculated using 14 basis functions. The columns in Table 1 are as  
161 follows: 1) the resonance number; 2) the experimental resonance frequencies ( $f_{ex}$ ); 3) resonance  
162 frequencies ( $f_r$ ) calculated from the fitting software; 4) percent error for each resonance,  $\%err =$   
163  $(f_r - f_{ex})/f_{ex} * 100$ ; 5) a weighting factor,  $wt$ , between 0 and 1 that indicates how heavily the fit  
164 procedure should consider each resonance (0 means do not consider, 1 means consider fully); 6)  
165 mode symmetry ( $k$ ) as described in Ref [Migliori and Sarrao]; 7) order ( $i$ ); and finally 8), the  
166 sensitivity of each resonance frequency to the elastic moduli normalized to unity ( $df/dC_{11}$  and  
167  $df/dC_{44}$ ).

168 The root mean square (rms) error of the fit ( $\sqrt{\sum_n \frac{(f_r - f_{ex})^2}{n}} \times 100$ ) shown in the table was  
169 0.33%, which gives a high confidence for the calculated values of elastic moduli. As seen in  
170 Table 1, two resonances, at 117.03 and 145.32 kHz, were omitted from the calculations. After  
171 multiple fitting attempts, these resonances were obvious outliers and could not be fit to better  
172 than 1%. Considering that Berea sandstone is a porous material, and the transducers were glued  
173 on the sample, it is not unexpected that some resonances will be affected more than others by  
174 these artifacts. RUS fits that included anisotropy were also investigated (cubic and hexagonal),  
175 but did not lead to significant improvement of the fit or to significant changes in determined  
176 elastic moduli. This finding indicates that the earlier-stated assumption that the sample is  
177 isotropic on these length scales is reasonable.

178 Once a stable fit was obtained, the room temperature dimensions of the sample were also  
179 allowed to vary, resulting in the following dimensions of the sample:  $9.05 \times 8.23 \times 6.81 \text{ mm}^3$ .  
180 These dimensions are different by about 1-2% compared to our measured values. Due to the  
181 porous nature of the material, the corners of the sample are not perfectly sharp. Allowing the  
182 dimensions to vary in the fitting routine accounts for this artifact to some extent. Thermal  
183 expansion of the sample was accounted for in calculation of the elastic moduli for each  
184 temperature step using available thermal expansion data [Somerton and Salim, 1961]. The  
185 volumetric thermal expansion was estimated as  $43.7 \cdot 10^{-6} \text{ K}^{-1}$  from figure 3 in the reference  
186 above.

187 The first 25 resonance modes for the sample used in this study are depicted graphically and  
188 in order (first left-to-right and then top-to-bottom) in Fig. 3. The graphical representations are  
189 calculated using COMSOL Multiphysics. For each mode, the instantaneous particle  
190 displacements are shown using a thermometer color scheme where blue is low (cold) and red is a  
191 high value (hot). No correlation between face displacement of poorly fitted modes and the face  
192 on which the transducers were mounted was found. This is illustrated by comparing table 1 to  
193 figure 3 in which poorly fitted modes had a degenerate mode that fit well.

194 The room temperature values of  $C_{11}$  and  $C_{44}$  were found to be 12.2 and 4.8 GPa, respectively.  
195 From these values and the density ( $\rho=2115 \text{ kg/m}^3$ ) determined from the measured mass and the  
196 fit dimensions of the sample, the following quantities of interest were calculated: bulk modulus  
197  $B = 5.8 \text{ GPa}$ , Young's modulus  $E = 11.32 \text{ GPa}$ , Poisson ratio  $\nu = 0.17$ , compressional sound  
198 speed  $v_P = 2402 \text{ m/s}$ , shear sound speed  $v_S = 1511 \text{ m/s}$  and  $v_P/v_S = 1.59$ .

199 The room temperature elastic constants  $C_{11}$  and  $C_{44}$  are within 12% of recently published  
200 data on Berea Sandstone [Remillieux *et al.*, 2015], which reports  $C_{11} = 10.86 \text{ GPa}$ , and  $C_{44} = 4.24$   
201 GPa. These values lead to similar values for Young's modulus,  $E = 10 \text{ GPa}$ , and Poisson's ratio,  
202  $\nu = 0.18$ . The compressional sound speed is in good agreement with Ref Shankland [Shankland  
203 *et al.*, 1993] and Renaud [Renaud *et al.*, 2013] who report values of  $v_P = 2380 \text{ m/s}$  and  $v_P = 2450$   
204 m/s, respectively. However, the values determined here differ by as much as 50% when  
205 compared to Winkler ( $v_P = 1930 \text{ m/s}$ ) [Winkler *et al.*, 1979] and Sayers ( $v_P = 3280-3600 \text{ m/s}$ )  
206 [Sayers *et al.*, 1990]. Such differences are common in the sandstone literature and can be  
207 attributed to different densities and/or porosities of the samples used in each individual study.

## 208 **3.2. Temperature Dependence**

209 All spectra versus temperature are plotted in figure 4. Each spectrum is plotted at its  
210 corresponding temperature with darker color indicating higher amplitude. For example, it can be  
211 seen that the most prominent resonance in Fig.2, at approximately 115 kHz, corresponds with the  
212 darkest line in Fig. 4. The strong curvature of the resonance position with respect to  
213 temperature shows that Berea sandstone has a very significant resonance shifting with  
214 temperature. Two prominent resonant frequencies versus temperature are plotted in Figure 5, and

215 show the characteristically strong dependence of resonant frequency on sample temperature  
216 mentioned above. The dependence of resonance frequency on temperature can be separated into  
217 two distinct regions. Between room temperature and 385 K, the Berea sandstone exhibit behavior  
218 of regular solids, i.e. softening as temperature increases. However, between 385 K and 478 K,  
219 the material is found to stiffen with temperature. For example, over the first 100 K, the  
220 resonances change by < -400 ppm/K. At ~385 K, the resonances begin increasing at a rate > 400  
221 ppm/K for the final 100 K considered here. This unexpected behavior was found to be  
222 repeatable upon thermal cycling. Additional through-transmission experiments were performed  
223 with separate, larger samples (24.80 x 15.86 x 15.86 mm) of Berea sandstone which confirmed  
224 the trends seen by these RUS experiments. The results of these experiments are not shown here.  
225 Mode stiffening with temperature is unusual and has been observed in few materials [e.g. *Pantea*  
226 *et al.*, 2006; *Wang et al.*, 2015; *Hancock et al.*, 2015].

227 A qualitative comparison of our data with Ulrich and Darling (Fig. 6) shows that Berea  
228 softens with temperature between 225 K and 385 K, as is typically found in solids. The  
229 anomalous stiffening with temperature can also be observed in the figure in two different  
230 temperature regions, <200 K and >375 K. Figure 7 presents the bulk modulus value ( $B =$   
231  $C_{11} - \frac{4}{3}C_{44}$ ) that was calculated from the determined elastic moduli at each temperature. A  
232 quantitative analysis of this data reveals an approximately 17% softening with temperature  
233 between room temperature and 385 K, followed by an almost equal percentage of stiffening  
234 between 385 K and 480 K. By comparing Fig. 7 with Figs. 4 & 5, it can be seen that the bulk  
235 modulus is ~4x more sensitive to changes in temperature than the individual resonance  
236 frequencies. This difference can be largely attributed to the fact that the resonance frequencies  
237 include a change not only in material stiffness, but also in physical dimension through the  
238 coefficients of thermal expansion. Young's modulus and Poisson ratio vary by about 8%, and  
239 19% respectively.

240 Compressional ( $C_{11}$ ) and shear ( $C_{44}$ ) elastic moduli have a similar qualitative temperature  
241 dependence and turnover temperature (Fig. 8). However,  $C_{11}$  can be seen to have a significantly  
242 larger quantitative temperature dependence, with a  $\pm 1000$  ppm/K variability compared to  $C_{44}$   
243 which has approximately half of that sensitivity, or  $\sim \pm 600$  ppm/K in the same temperature  
244 ranges. Considering that Berea sandstone is composed largely of  $SiO_2$  it is perhaps interesting to  
245 compare the temperature derivatives of the elastic moduli determined here to the well-known  
246 values of these quantities for  $\alpha$ -quartz [Bechmann *et al.*, 1962]. Around room temperature, the  
247 compressional elastic moduli of  $\alpha$ -quartz,  $C_{11}$  and  $C_{33}$ , have first order temperature coefficients  
248 ( $\frac{1}{C_{xx}} \frac{dC_{xx}}{dT}$ ) of -49 ppm/K and -160 ppm/K, respectively. These values are remarkably smaller  
249 than the -1000 ppm/K for  $C_{11}$  mentioned above. The shear moduli for  $\alpha$ -quartz have temperature  
250 coefficients ranging from -177 ppm/K for  $C_{44}$  to +178 ppm/K for  $C_{66}$  [Bechmann *et al.*, 1962].

251 The great span of values for the temperature coefficients for the  $\alpha$ -quartz shear moduli  
252 likely reflects little more than the fact that it is highly anisotropic (belonging to crystal point

253 group 32) while the Berea sample studied here is assumed isotropic. However, that both  
254 compressional moduli of  $\alpha$ -quartz are 3-20 times less sensitive to temperature appears to be more  
255 significant. This result reinforces the intuitive belief that the mechanical properties of the  
256 constituents of a macroscopic composite such as Berea have little bearing on the mechanical  
257 properties of the composite, itself.

258 **4. Summary**

259 Resonant Ultrasound Spectroscopy was used for determination of the elastic moduli of  
260 dry Berea sandstone, both at room temperature and at high temperatures characteristics to depths  
261 of about 8 km. Sample dimensions were chosen to be relatively small, less than 1 cm on every  
262 side, in order to avoid complications brought by low frequencies and to minimize the effects of  
263 anisotropy. Room temperature data show that Berea sandstone is a very soft material, with a bulk  
264 modulus of only 5.8 GPa. It was found that Berea sandstone undergoes a softening between  
265 room temperature and 385 K, followed by an abnormal behavior of stiffening between 385 K and  
266 478 K.

267 **Acknowledgements**

268 The authors thank T.J. Ulrich for helpful discussions. This work was partially funded by the U.S.  
269 Dept. of Energy. All data found in the results section of this paper is available upon request from  
270 the corresponding author.

271

272

## References

273 Bechmann, R., A. D. Ballato, and T.J. Lukaszek (1962), Higher-Order Temperature Coefficients  
 274 of the Elastic Stiffnesses and Compliances of Alpha-Quartz, *Proceedings of the IRE*,  
 275 50(8), 1812-1822, doi: 10.1109/JRPROC.1962.288222

276 Costin, L. S., and D. J. Holcomb (1981), Time-dependent failure of rock under cyclic  
 277 loading. *Tectonophysics*, 79(3), 279-296, doi: 10.1016/0040-1951(81)90117-7.

278 Finger, J., and D. Blankenship (2010), Handbook of best practices for geothermal  
 279 drilling. *Sandia National Laboratories, Albuquerque*.

280 Green, D. H., and H. F. Wang (1994), Shear wave velocity and attenuation from pulse-echo  
 281 studies of Berea sandstone, *J. Geophys. Res.*, 99(B6), 11755–11763,  
 282 doi:10.1029/94JB00506.

283 Hancock, J.C., K. W. Chapman, G. J. Halder, C. R. Morelock, B. S. Kaplan, L. C. Gallington, A.  
 284 Bongiorno, C. Han, S. Zhou, and A. P. Wilkinson (2015), Large Negative Thermal  
 285 Expansion and Anomalous Behavior on Compression in Cubic  $\text{ReO}_3$ -Type  $\text{A}^{\text{II}}\text{B}^{\text{IV}}\text{F}_6$ :  
 286  $\text{CaZrF}_6$  and  $\text{CaHfF}_6$ , *Chemistry of Materials*, doi: 10.1021/acs.chemmater.5b00662.

287 Harris, J. M., Y. Quan, and C. Xu (2005), Differential Acoustical Resonance Spectroscopy: An  
 288 experimental method for estimating acoustic attenuation of porous media. In *2005 SEG  
 289 Annual Meeting*. Society of Exploration Geophysicists, doi: 10.1190/1.2147992.

290 Hart, D. J., and H. F. Wang (1995), Laboratory measurements of a complete set of poroelastic  
 291 moduli for Berea sandstone and Indiana limestone. *Journal of Geophysical Research: Solid Earth* (1978–2012), 100(B9), 17741-17751, doi: 10.1029/95JB01242.

293 Johnson, P. A., R. A. Guyer, and L. A. Ostrovsky (1999), A nonlinear mesoscopic elastic class of  
 294 materials. *AIP Conference Proceedings*, 524, 291-294, doi:  
 295 <http://dx.doi.org/10.1121/1.427349>.

296 Johnson, P. A., B. Zinszner, P. Rasolofosaon, F. Cohen-Tenoudji, and K. Van Den Abeele  
 297 (2004), Dynamic measurements of the nonlinear elastic parameter  $\alpha$  in rock under  
 298 varying conditions, *J. Geophys. Res.*, 109, B02202, doi: 10.1029/2002JB002038.

299 Lebedev, A. V. (2002), Method of linear prediction in the ultrasonic spectroscopy of  
 300 rock. *Acoustical Physics*, 48(3), 339-346, doi: 10.1134/1.1478120.

301 Liang, W. G., Y. S. Zhao, S. G. Xu, and M. B. Dusseault (2011), Effect of strain rate on the  
 302 mechanical properties of salt rock. *International Journal of Rock Mechanics and Mining  
 303 Sciences*, 48(1), 161-167, doi: 10.1016/j.ijrmms.2010.06.012.

304 Liu, Y., H. Wu, C. T. Liu, Z. Zhang, and V. Keppens (2008), Physical factors controlling the  
305 ductility of bulk metallic glasses. *Applied Physics Letters*, 93(15), 151915, doi:  
306 <http://dx.doi.org/10.1063/1.2998410>

307 Migliori, A., and J. L. Sarrao (1997), *Resonant ultrasound spectroscopy: applications to physics,*  
308 *materials measurements, and nondestructive evaluation*. Wiley-Interscience

309 Nobili, M., M. Scalerandi, and P. P. Delsanto (2005), Temperature dependence of the elastic  
310 properties of hysteretic materials. In *Materials Science Forum* (Vol. 480, pp. 573-578),  
311 doi: 10.4028/www.scientific.net/MSF.480-481.573

312 Pandey, C. S., and J. Schreuer, (2012), Elastic and piezoelectric constants of tourmaline single  
313 crystals at non-ambient temperatures determined by resonant ultrasound  
314 spectroscopy. *Journal of Applied Physics*, 111(1), 013516, doi:  
315 <http://dx.doi.org/10.1063/1.3673820>.

316 Pantea, C., A. Migliori, P. B. Littlewood, Y. Zhao, H. Ledbetter, J. C. Lashley, T. Kimura, J.  
317 Van Duijin, and G. R. Kowach (2006), Pressure-induced elastic softening of  
318 monocrystalline zirconium tungstate at 300 K. *Physical Review B*, 73, 214118, doi:  
319 <http://dx.doi.org/10.1103/PhysRevB.73.214118>.

320 Remillieux, M., C., T.J. Ulrich1, C. Payan, J. Rivière, C. R. Lake1, P.-Y. Le Bas (2015),  
321 Resonant ultrasound spectroscopy for materials with high damping and samples of  
322 arbitrary geometry. *J. Geophys. Res.: Solid Earth, accepted manuscript*, doi:  
323 10.1002/2015JB011932.

324 Renaud, G., J. Rivière, P.-Y. Le Bas, and P. A. Johnson (2013), Hysteretic nonlinear elasticity of  
325 Berea sandstone at low-vibrational strain revealed by dynamic acousto-elastic testing,  
326 *Geophys. Res. Lett.*, 40, 715–719, doi: 10.1002/grl.50150.

327 Sayers, C. M., J. G. Van Munster, and M. S. King (1990), Stress-induced ultrasonic anisotropy  
328 in Berea sandstone. In *International Journal of Rock Mechanics and Mining Sciences &*  
329 *Geomechanics Abstracts* (Vol. 27, No. 5, pp. 429-436), doi:10.1016/0148-  
330 9062(90)92715-Q

331 Sedmák, P., H. Seiner, P. Sedlák, M. Landa, R. Mušálek, and J. Matějíček (2013), Application of  
332 resonant ultrasound spectroscopy to determine elastic constants of plasma-sprayed  
333 coatings with high internal friction. *Surface and Coatings Technology*, 232, 747-757, doi:  
334 10.1016/j.surfcoat.2013.06.091

335 Shankland, T. J., P. A. Johnson, and T. M. Hopson (1993), Elastic wave attenuation and velocity  
336 of Berea sandstone measured in the frequency domain. *Geophysical Research*  
337 *Letters*, 20(5), 391-394, doi: 10.1029/92GL02758

338 Slatt, R. M. (2013), Stratigraphic Reservoir Characterization for Petroleum Geologists,  
339 Geophysicists, and Engineers. *Developments in Petroleum Science*, 61, Elsevier.

340 Somerton, W. H., and M. A. Selim (1961), Additional thermal data for porous rocks—thermal  
341 expansion and heat of reaction. *Soc. Pet. Engrs*, <http://dx.doi.org/10.2118/1613-G>.

342 Ten Cate, J. A., and T. J. Shankland (1996), Slow dynamics in the nonlinear elastic response of  
343 Berea sandstone. *Geophysical Research Letters*, 23(21), 3019-3022, doi:  
344 10.1029/96GL02884.

345 Ulrich, T. J., and T. W. Darling (2001), Observation of anomalous elastic behavior in rock at low  
346 temperatures. *Geophysical Research Letters*, 28(11), 2293-2296, doi:  
347 10.1029/2000GL012480

348 Wang L, et al., Metal fluorides, a new family of negative thermal expansion materials, *Journal of  
349 Materomics* (2015), <http://dx.doi.org/10.1016/j.jmat.2015.02.001>

350 Wang, S. X., J. G. Zhao, Z. H. Li, J. M. Harris, and Y. Quan (2012), Differential Acoustic  
351 Resonance Spectroscopy for the acoustic measurement of small and irregular samples in  
352 the low frequency range. *Journal of Geophysical Research: Solid Earth* (1978–  
353 2012), 117(B6), doi: 10.1029/2011JB008808.

354 Winkler, K., A. Nur, M. Gladwin (1979), Friction and Seismic Attenuation in Rocks. *Nature*,  
355 277, 528-531, doi: 10.1038/277528a0.

356 Winkler, K. W. (1983), Frequency dependent ultrasonic properties of high-porosity sandstones,  
357 *J. Geophys. Res.*, 88(B11), 9493–9499, doi: 10.1029/JB088iB11p09493.

358 Zhang, J. J., and L. R. Bentley (2003), Pore geometry and elastic moduli in sandstones.  
359 *CREWES, University of Calgary*.

360

361

362

363

364

365

366

367

368

## Tables

369

**Table 1.** Room Temperature RUS Fit of Berea Sandstone

370

n	f <sub>ex</sub> (kHz)	f <sub>r</sub> (kHz)	%err	wt	k	i	df/dC <sub>11</sub>	df/dC <sub>44</sub>
1	72.59	72.85	0.35	1.00	4	1	0.00	1.00
2	96.83	96.91	0.08	1.00	6	2	0.22	0.78
3	100.81	100.49	-0.32	1.00	4	2	0.00	1.00
4	103.40	103.35	-0.05	1.00	7	2	0.32	0.68
5	108.56	108.90	0.32	1.00	3	2	0.04	0.96
6	114.11	113.95	-0.14	1.00	6	3	0.62	0.38
7	117.03	118.28	1.07	0.00	1	2	0.27	0.73
8	120.02	120.05	0.03	1.00	2	2	0.03	0.97
9	122.98	122.19	-0.65	1.00	5	1	0.06	0.94
10	124.51	124.35	-0.13	1.00	8	2	0.04	0.96
11	129.25	128.82	-0.33	1.00	8	3	0.28	0.72
12	131.61	131.16	-0.34	1.00	5	2	0.20	0.80
13	132.88	132.97	0.07	1.00	2	3	0.33	0.67
14	139.59	139.63	0.03	1.00	5	3	0.24	0.76
15	145.32	147.95	1.81	0.00	7	3	0.47	0.53
16	151.75	150.84	-0.60	1.00	1	3	0.51	0.49
17	152.52	152.47	-0.04	1.00	8	4	0.04	0.96
18	154.67	154.15	-0.34	1.00	5	4	0.59	0.41
19	156.80	156.93	0.09	1.00	3	3	0.35	0.65
20	159.09	159.99	0.56	1.00	5	5	0.67	0.33
21	163.73	164.19	0.28	1.00	4	3	0.16	0.84
22	165.76	165.38	-0.23	1.00	6	4	0.24	0.76
23	166.03	166.29	0.16	1.00	2	4	0.05	0.95
24	168.61	169.21	0.36	1.00	1	4	0.10	0.90
25	169.58	169.74	0.10	1.00	7	4	0.14	0.86

382

383

384

385

386 **Figures**



**Figure 1.** The LiNbO<sub>3</sub> transducers attached to opposing faces of the 9.13 x 6.65 x 8.32 mm Berea sandstone sample using high temperature epoxy

387

388

389

390

391

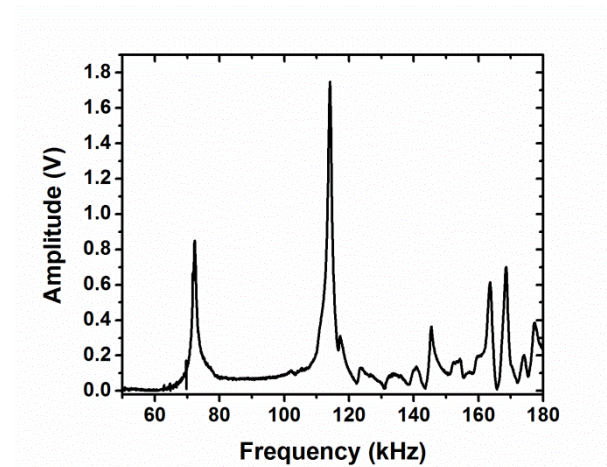
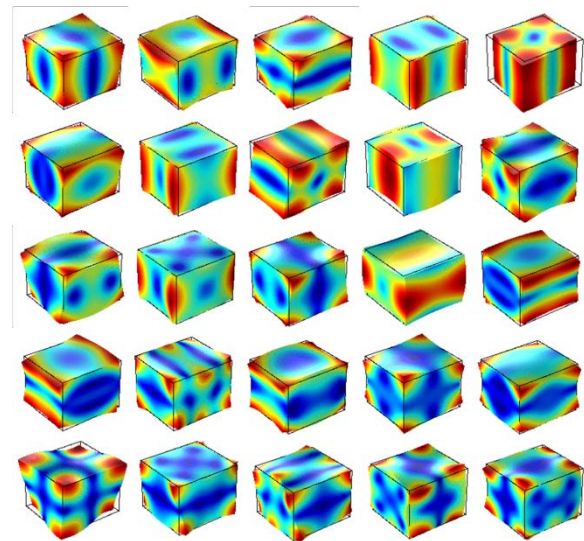


**Figure 2.** A typical RUS spectrum collected in this study, at room temperature

392



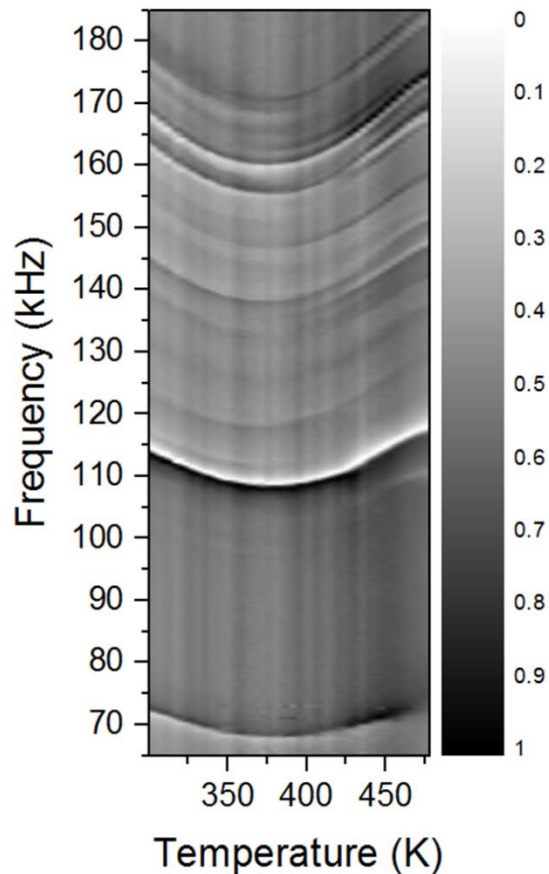
393

394

**Figure 3.** Resonance modes for Berea sandstone at room temperature – modes are in order

395

396



397

**Figure 4.** Resonance spectra for each temperature step. The amplitudes are normalized to the highest amplitude at each temperature. Higher amplitudes are designated by darker color.

398

399

400

401

402

403

404

405

406

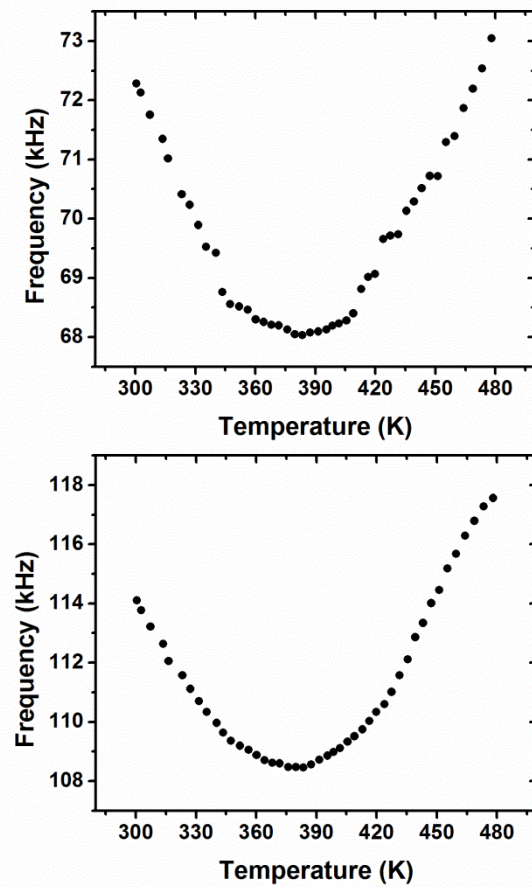


**Figure 5.** The 1<sup>st</sup> and 2<sup>nd</sup> most prominent resonance frequencies (see Fig. 2) plotted vs temperature.

407

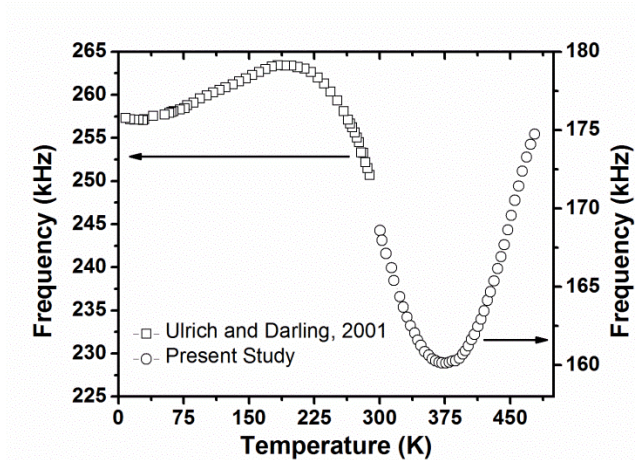


**Figure 6.** One resonant frequency from this study plotted versus temperature together with frequency data from Ulrich and Darling

408

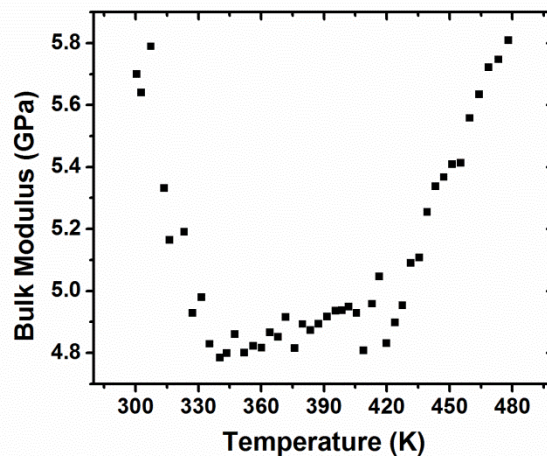


**Figure 7.** Calculated bulk modulus at each temperature

409

410

411

412

413

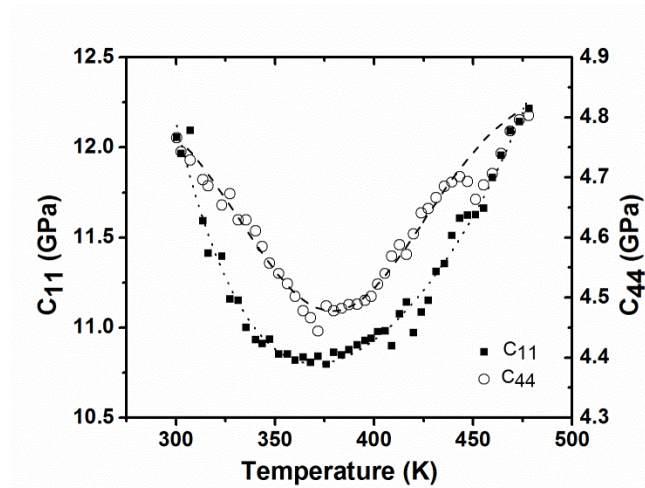


**Figure 8.** Independent elastic moduli C11 and C44 plotted vs temperature. Lines are to guide the reader's eyes